Journal of Geoscience and Environment Protection, 2022, 10, 198-228
https://www.scirp.org/journal/gep
ISSN Online: 2327-4344
ISSN Print: 2327-4336

Magmatism of the Beka Volcanic Massifs (Cameroon Volcanic Line, West-Central Africa): New Petrographical and Mineralogical Data

Jacques Dili-Rake[1,2*], Sahabo Aboubakar Abdoulaye[1,2], Joseph Legrand Tchop[1], Merlin Isidore Teitchou[1], Christian Mana Bouba[3], Oumarou Faarouk Nkouandou[4], Daouda Dawaï[2], Eddy Ferdinand Mbossi[1]

[1]Research Centre for Geophysics and Volcanology, Institute of Geological and Mining Research, Buea, Cameroon
[2]Faculty of Sciences, University of Maroua, Maroua, Cameroon
[3]Centrer for geological and Mining Research, Institute of Geological and Mining Research, Garoua, Cameroon
[4]Faculty of Sciences, University of Ngaoundere, Ngaoundere, Cameroon
Email: *dilirakejacques@yahoo.fr

How to cite this paper: Dili-Rake, J., Abdoulaye, S. A., Tchop, J. L., Teitchou, M. I., Bouba, C. M., Nkouandou, O. F., Dawaï, D., & Mbossi, E. F. (2022). Magmatism of the Beka Volcanic Massifs (Cameroon Volcanic Line, West-Central Africa): New Petrographical and Mineralogical Data. *Journal of Geoscience and Environment Protection, 10,* 198-228.
https://doi.org/10.4236/gep.2022.107013

Received: June 21, 2022
Accepted: July 23, 2022
Published: July 26, 2022

Abstract

The Beka volcanic massifs are located northeast of Ngaoundere region, within the Adamawa plateau. It consists mainly of basanites, trachytes and phonolites. The petrographic study shows that all the basanite lavas have porphyritic microlitic textures with a more pronounced magmatic fluidity than the felsic lavas displaying trachytic textures. The lavas are composed of phenocrysts, microlites and microphenocrysts of olivine, clinopyroxene, plagioclase and iron-titanium oxides for the basanites and of greenish clinopyroxene, alkali feldspar, and titanomagnetite for the felsic lavas. Chemical microprobe analysis indicates that the olivine crystals are magnesian ($Fo_{73\text{-}78}$). Clinopyroxene crystals have a composition of diopside ($Wo_{47\text{-}}$) in the basaltic lavas and diopside near the hedenbergite pole in the trachytes phonoliths and titanomagnetite (TiO_2: 21.13% - 22.36% and FeO: 68% - 68%). Chemical analyses on whole rocks show that all the lavas belong to the same series and the felsic lavas come from the differentiation of basanite lavas by fractional crystallization of the minerals therein. The basanites originate from a low rate of partial melting of an OIB-type mantle. Contamination and mixing processes are suspected. Lavas of similar composition are found in other volcanic centres of the Adamawa plateau and the continental and oceanic sectors of the Cameroon Volcanic Line, in particular the Kapsiki plateau, Mounts Cameroon and Bamenda.

Keywords

Cameroon Volcanic Line, Adamawa Plateau, Beka Volcanic Massif,

Fractional Crystallization, OIB-Type Mantle

1. Introduction and Geological Setting

The Adamawa plateau belongs to the Cameroon Volcanic Line. The relationship between the CVL and the Adamawa Plateau remains complex. However, the origin of the Cameroon Volcanic Line (CVL) remains the subject of much debate. Several hypotheses have been put forward on this subject: 1) According to the model of Freeth (1979) and Browne & Fairhead (1983), a rapid rotation 20 Ma ago between 8˚ and 9˚ of the African plate would have induced an inflection of the CVL which extends from the Gulf of Guinea and progressively curves from N30˚E to N70˚E on the Adamawa plateau. 2) Fitton (1983) suggested a 7˚ rotation of the African plate from a pole in Sudan 80 Ma ago (Santonian), which would have cut the lithosphere of the Benue trough and moved it to the present geographical location of the CVL. 3) According to Ashwal & Burke (1989), they would be related to the reactivation of the Pan-African crust, and the orientation of the dyke swarms could result from the reworked Pan-African fault network of the Adamawa Plateau (Moreau et al., 1987) during several Ordovician (450 Ma) and Jurassic episodes; 4) Fairhead & Okereké (1988) suggested the development of the West and Central African rift systems. 5) Ngangom et al. (1983) mentioned the development of the Cretaceous Djerem and Mbere basins of northern Cameroon. These hypotheses are plausible from a structural point of view, but remain difficult to establish from a petrological point of view. Based on field, mineralogical and geochemical investigations, the present study aims to highlight the nature, genesis and determines the magmatic relation between the observed Beka lavas. The signification of these lavas in the context of CVL is also debated by comparing with other volcanic occurrences of this line.

The Adamawa Plateau (**Figure 1**) is a pan-African metamorphic and plutonic basement horst bounded to the north by the Adamawa Fault and to the south by the Djerem and Mbere faults (Dumont, 1987). It is intensely affected by a network of major N70˚E faults locally masked by Cenozoic basaltic flows (Moreau et al., 1987). The main fault that crosses it, named the Adamawa Fault, represents one of the structures that cross Africa from West to East (Cornacchia & Dars, 1983). This area was the site of significant Mid-Pliocene volcanic activity (Gouhier et al., 1974; Oustriere, 1984; Deruelle et al., 1987; Nkouandou et al., 2008). Volcanic eruptions have created high massifs such as Tchabal Nganha (Nono et al., 1994), Tchabal Djinga (Ménard et al., 1998) and Tchabal Mbabo (Fagny et al., 2020). Effusive flows of alkaline basalts have contributed to the formation of uneven relief on the plateau to the north and the east of Ngaoundere town (Nkouandou et al., 2010). Other petrographic (Nono et al., 1994; Temdjim et al., 2004; Nkouandou et al., 2010), geophysical (Poudjom Djomani et al., 1997) and structural (Dumont et al., 1987; Cornacchia & Dars, 1983;

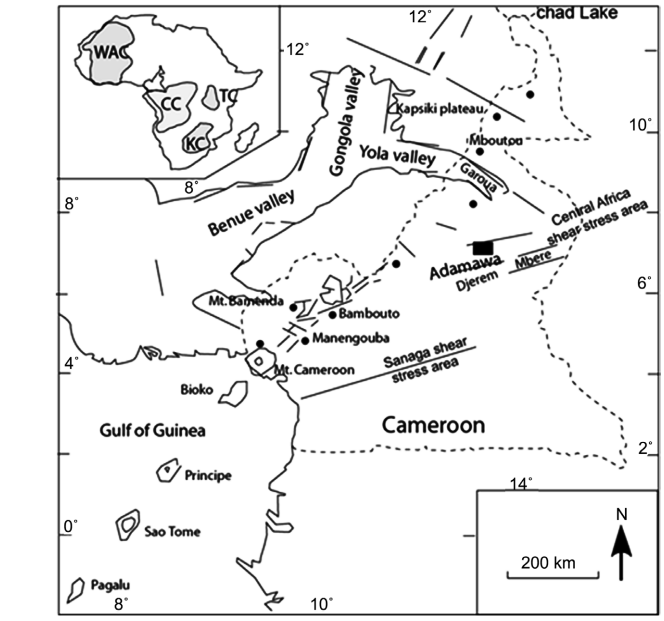

(a)

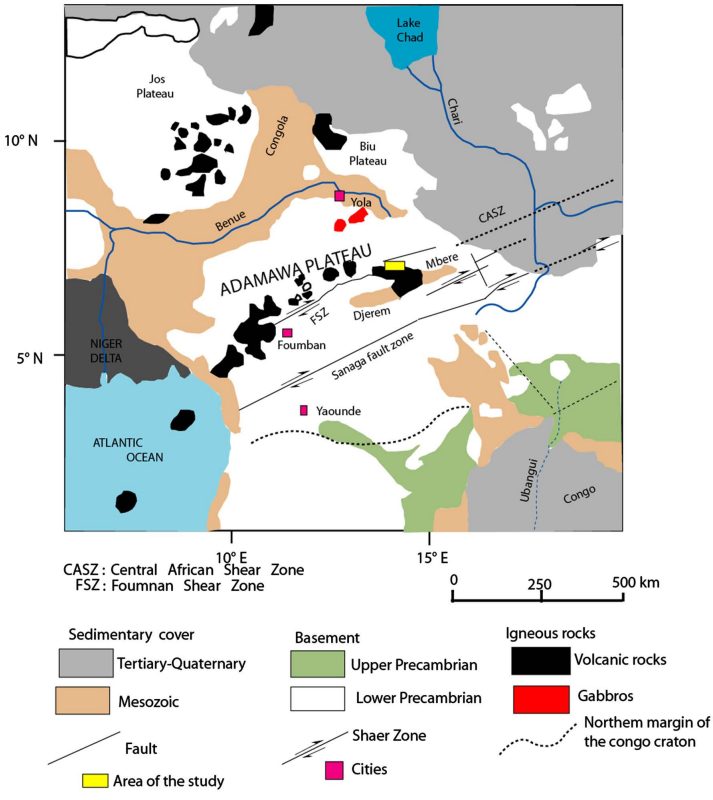

(b)

Figure 1. (a) Location of the study area (black rectangle) in the Adamawa Plateau in relation to the Cameroon Volcanic Line. (b) Main geological features in the Adamawa Plateau. The Djerem graben, the main volcanic and plutonic complexes are from (Déruelle et al., 2007) as well as the Central Cameroon Shear Zone is after Ngako et al. (2006) and Central African shear zone (Guiraud et al., 1992). The Cratons fields are after (Kampunzu & Popoff, 1991). WAC: West Africa Craton; CC: Congo Craton; CT: Tanzania Craton; KC: Kalahri Craton.

Ganwa et al., 2008) studies have also helped characterise the Adamawa basement.

The Adamawa Plateau basement is intensely dissected by the Pan-African faults trending N70˚E (Moreau et al., 1987), which were remobilised during the Albian-Aptian period, exposing numerous types of volcanic rocks: basanite, basalt, hawaiite, mugearite, benmoreite, trachyte, rhyolite, phonolite. The differentiated lavas show peralkaline affinities (Nkouandou et al., 2008, 2015; Fagny et al., 2012).

The volcanic formations in the vicinity of Ngaoundere have been grouped into three successive emission series (Guiraudie, 1955; Lasserre, 1961) and in accordance with the observations of (Gèze, 1943) in western Cameroon: 1) the ancient basaltic series of terminal Cretaceous (Lasserre, 1961); 2) the intermediate trachytic and phonolitic-dominated series of Tortonian period and 3) the recent basaltic series.

The trachytic and phonolitic dominated series is represented by 35 necks, domes and dome flows of differentiated lavas associated with basaltic flows of Mio-Pliocene basalt age (10.0 to 7.0 ± 0.2 Ma, Temdjim et al., 2004; Nkouandou et al., 2008, 2010) and differentiated lavas (11.39 ± 0.03 to 9.28 ± 0.03, Marzoli et al., 1999). The basalts contain peridotite nodules. Two large strato-volcanoes; Tchabal Nganha (Nono et al., 1994; Fagny et al., 2016) and Djinga-Tadorgal (Mbowou et al., 2010) consist of basaltic, trachytic, phonolitic flows and volcanic breccias, crossed by numerous trachytic and phonolitic necks. One basalt and two trachytes have been dated K-Ar at 7.2 - 7.9 and 7.9 - 9.8 (±0.2) Ma, respectively (Gouhier et al., 1974).

The Adamawa Plateau was formed during the Tertiary period and then raised up to 1 km from the surrounding areas (Okereke, 1988). It is largely covered by large basaltic and basalt-andesitic volcanic outpourings of mainly Tertiary age, which spill over into the middle part of the southern trough (Le Maréchal & Vincent, 1971). The plateau is then also presented as a volcanic horst about 200 km wide, bounded to the north and south, as mentioned above, by pan-African faults, generally oriented N70˚E. Depending on the author, the volcanism of the Adamawa Plateau remains a matter of debate. It either belongs to the Cameroon Volcanic Line (CVL) or is rather related to pan-African fault replay, resulting from the reactivation of the N70˚E sinistral trans-tensional shear zone, at the beginning of the opening of the central Atlantic Ocean in the Aptian-Albian age (Moreau et al., 1987) and the separation of Africa and South America (Gouhier et al., 1974; Aka et al., 2009).

2. Analytical Methods

After field investigations, fresh representative samples were selected and six thin sections were prepared at the GEOPS Laboratory (Geosciences-Environment Laboratory of the University of Paris Saclay) in France. Mineralogical analyses (olivine, clinopyroxene, plagioclase and iron-titanium oxides) of the studied la-

vas were carried out with the SX100 microanalyser at the department of Pierre and Marie Curie University, Paris XI. The analytical conditions are specific to the minerals and take into account their structure, their stability under the electron beam and the elements sought.

Whole rock (major, trace and rare earth elements) geochemical analyses were carried on representative lavas using ICP-AES (Inductively Coupled Plasma-Atomic Emission Spectrometry) and ICP-MS (Inductively Coupled Plasma-Mass Spectrometry) at the laboratory of the CRPG of Nancy. After each sample, the grinder was systematically cleaned with compressed air. These analyses were carried out on 0.2 g of rock powder and the analytical accuracies varied between 0.04% and 0.1% for major elements and 0.1 to 0.5 ppm for trace and rare earth elements. The loss on ignition was determined by the weight difference after ignition at 1000˚C.

3. Results

3.1. Geological Setting of the Beka Area

Rocks within the Beka area comprise basanites, trachytes and phonolites (**Figure 2**). The basanite lavas outcrop as flows and as domes, at an altitude of 1272 m, with a height of 62 m and a diameter of approximately 270 m (**Figure 3(a)**). The basanite dome consists of the first few meters of the base, centimetric (35 to 80 cm) to metric (1 to 1.3 m) blocks and centimetric balls (15 to 80 cm) (**Figure 3(a)**). The blocks have rough surfaces with coarse centimetric to metric pyroxene crystals comparable to charcoal platelets. The balls, on the other hand, have a smooth surface and present rare pyroxene and olivine crystals on the surface. The upper part consists entirely of highly prismatic lavas, some of which are in the form of lauzes.

Trachytes occur as a 300 m × 150 m dome, culminating at an altitude of 1280 m with a height of 110 m above the basement (**Figure 3(b)**). The lava is dark green to greyish when ongoing alteration. It is covered by an approximately (1.5 to 5 cm) whitish to light yellow weathered patina. The fresh matrix has a pisolitic structure characterized by dark concretions consisting of mineral aggregates of variable diameter (0.5 to 1.5 cm).

The phonolite massif is a roughly conical dome, with steep slopes and almost circular base (**Figure 3(c)**). It rises to an altitude of 1314 m, and is 12 m high above the basement with a diameter of about 300 m. The massif is strongly prismatic. The prisms, mechanically degraded, show intense fracturing, due to climatic variations. The lava is characterized by the presence of dark grey spherical balls with diameter of 0.5 - 2 cm (**Figure 3(c)**).

The Beka volcano was developed on a slightly south-facing plateau and is represented by the conical and elongated domes and dome flows respectively.

The WNW-ESE cross section (**Figure 4**), based on the geological map of the study area (**Figure 2**), also enabled us to define the main morphological features of the Beka area. The landscape is made up of conical domes and hills whose

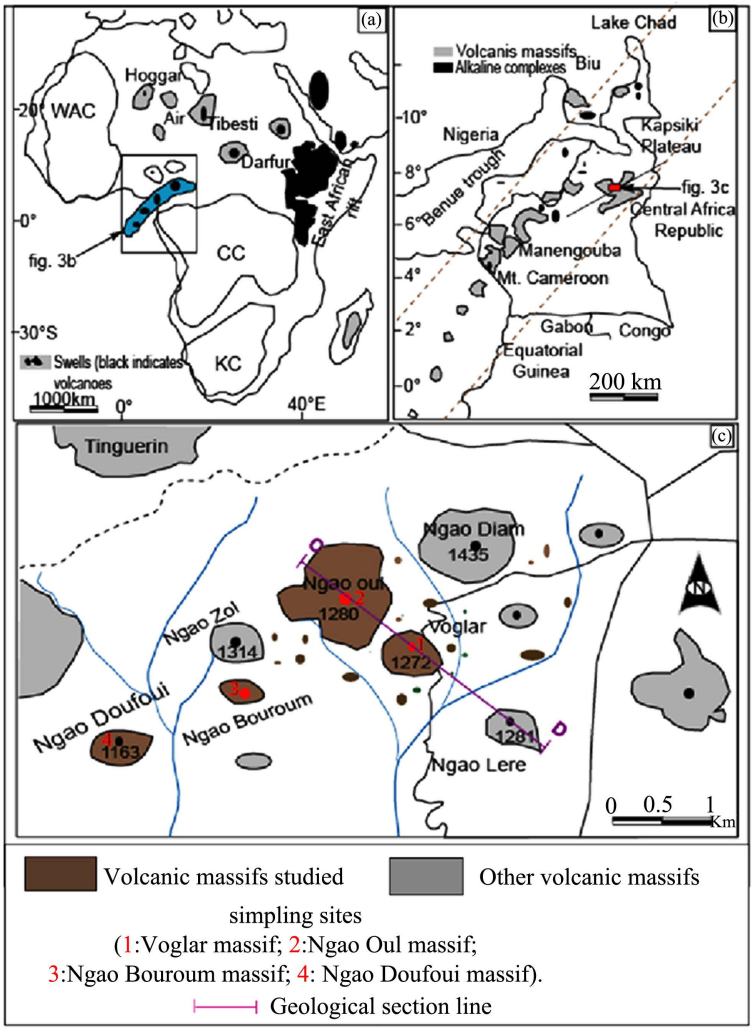

Figure 2. (a) Location map of the Cameroon Volcanic Line (CVL); (b) Main geological features of Africa and alkaline volcanic complexes of CVL. Central Cameroon Shear Zone is after Ngako et al. (2006); (c) Simplified geological map of the studied area with sampling sites.

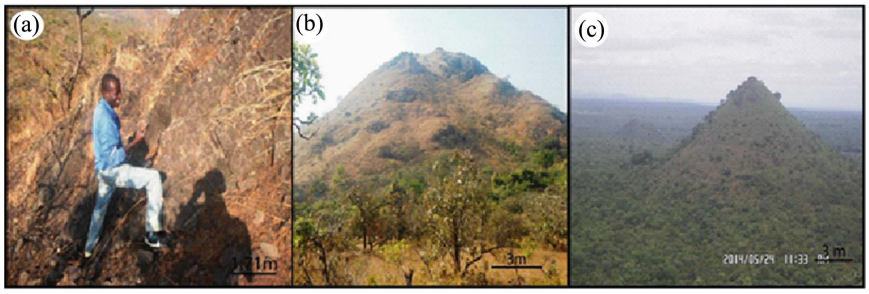

Figure 3. Panoramic view of the Beka outcrops and its surroundings, (a) Prismatic volcanic massif in its upper part; (b) Trachytic flow dome; (c) Phonolite massif.

slopes can easily reach 7%. The slopes have large incisions which have been heavily carved by torrents and unevenly shaped by slabs, balls and blocks of granitic basement.

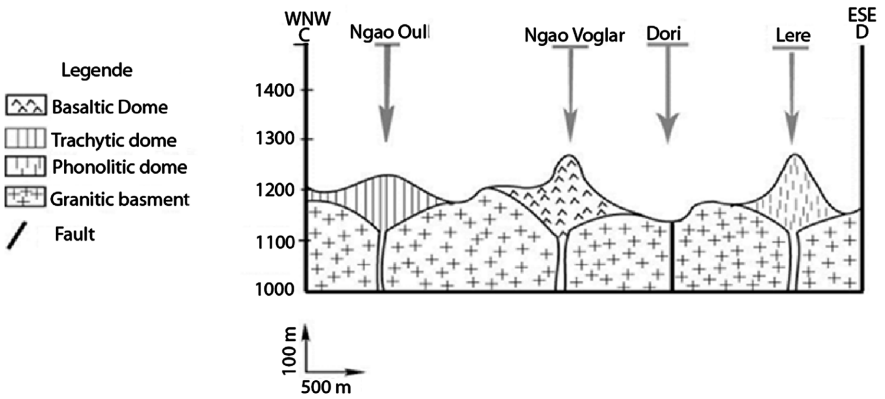

Figure 4. Sketch of the geological section illustrating the emplacement of Beka volcanism, based on the geological and topographic maps of the study area.

3.2. Petrography

3.2.1. Basanites

Basanites generally have a microlitic porphyritic texture and are made up of olivine, clinopyroxene, feldspar and iron-titanium oxides. The phenocrystalline phase is characterized by phenocrysts of olivine, clinopyroxene and iron-titanium oxides (Figure 5(a)). All these phenocrysts are distributed in a mesostasis consisting of microlites of the same minerals, i.e. microcrystals of iron-titanium oxides, pyroxene, olivine and microlites of plagioclase.

The olivine phenocrysts (0.5 × 0.3 mm, 5 - 10 vol%) are euhedral to subhedral. They are corroded along the rims and sometimes in the cores (Figure 5(b)). Rare inclusions of iron-titanium oxides are observed in these phenocrysts. Some of them show corrosion gulfs in the cores, although they are not very pronounced. Other olivine crystals are serpentinized and exhibit a yellowish alteration product in the cracks (Figure 5(b)).

Clinopyroxene phenocrysts (1 × 0.4 mm, 10 - 15 vol%) are automorphic and occur in various forms: elongated, and sometimes rectangular (Figure 5(b)). Some clinopyroxene crystals are strongly cracked and occasionally show marked corrosion gulfs in the core and/or along the rims occupied by iron-titanium oxides (Figure 5(a)).

Phenocrysts of iron-titanium oxides (0.4 × 0.3 mm) are in very low percentage (less than 8 vol%). They are generally associated to the olivine and clinopyroxene phenocrysts (Figure 5(b)).

The mesostasis of the studied basalts consists of plagioclase and clinopyroxene microlites and microcrystals of olivine and iron-titanium oxides. No preferential orientation of the microlites is observed.

The iron-titanium oxide microcrystals are relatively abundant (5% - 10% vol%) in the matrix. They are in the form of dotted lines and fine dark squares (Figure 5(b)). Olivine microcrystals are the least represented in the mesostasis (less than 2% vol%). They are mostly observed around phenocrysts of the same phase.

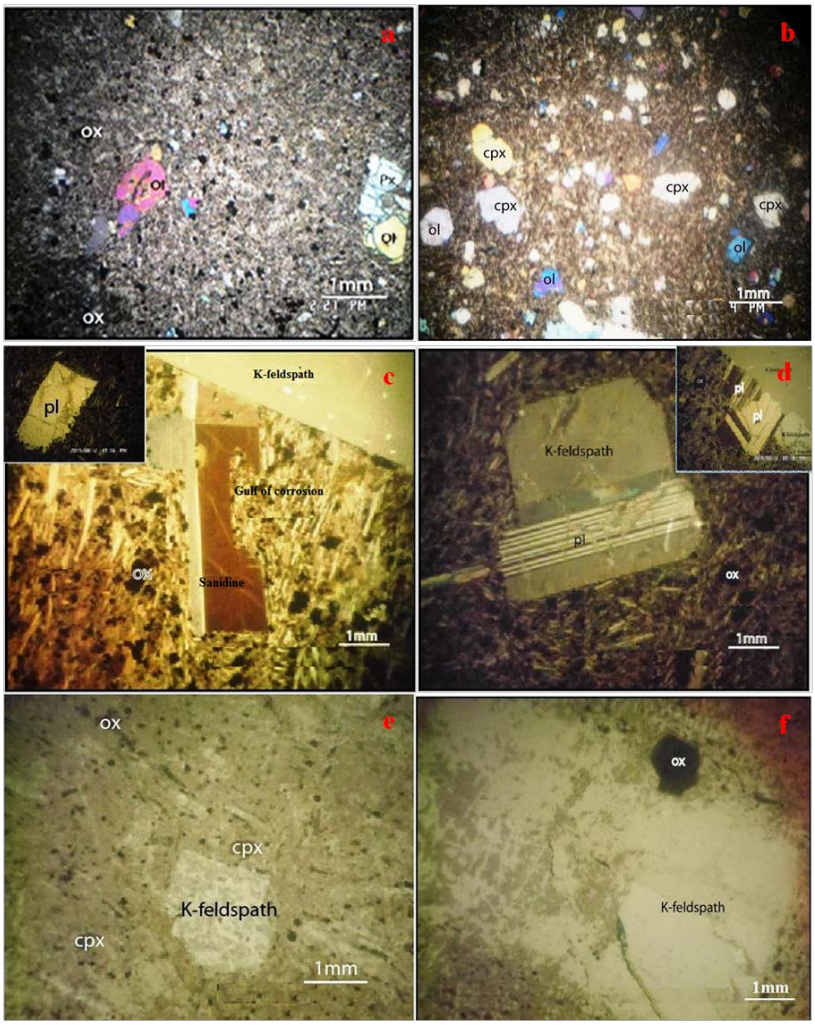

Figure 5. Microphotographs of thin sections of representative samples from the study area: (a) Destabilised phenocrysts of olivine in basanites; (b) Microlitic porphyritic texture of basanites; (c) Destabilised sanidine crystals in its core; (d) Trachytic texture of trachytic lavas; (e) and (f) Microlitic porhyric texture of phonolitic lavas.

Plagioclase microlites are the most abundant (10 - 15 vol%). They are elongated, appearing in the form of needles or rods of less than 1 mm for the most developed crystals. Clinopyroxene microlites (less than 0.5 mm, and 3 - 5 vol%) are lobate in the form of small elongated laths.

3.2.2. Trachytes

The thin sections of the trachyte samples have a classical trachytic texture. They are generally composed of phenocrysts of clinopyroxene, alkali feldspar, plagioclase and iron-titanium oxides. These phenocrysts are distributed in a microlitic matrix composed mainly of plagioclase, clinopyroxene and iron-titanium oxide microcrystals. Alkali feldspar phenocrysts (1.5 × 1 mm, 15% - 20% by volume of the rock) occur as elongated, automorphic platelets. They can reach 20% of the volume of the rock. They are sometimes cracked, destabilized Plagioclase phenocrysts (1.5 × 1 mm, 20% to 25% by volume of the rock) are automorphic

and others have a xenomorphic appearance. The latter are sometimes corroded in their edges by mesostasis and contain numerous microcrystals of iron-titanium oxides in these edges (Figure 5(c)). Clinopyroxene phenocrysts (1.2 × 0.8 mm) occupy about 10% by volume of the rock. They are automorphic to subautomorphic, cracked and sometimes corroded at the edges by mesostasis. They contain inclusions of iron-titanium oxide crystals and are sometimes completely altered to a brownish product (Figure 5(c)).

The mesostasis of the trachytic lavas consists mainly of plagioclase, clinopyroxene and iron-titanium oxide microcrystals. The iron-titanium oxide microcrystals are less than 0.1 mm in size, and occupy about 10% by volume of the rock. They are present in the matrix and or as inclusions in plagioclase phenocrysts (Figure 5(d)). Alkali feldspar microlites are the most abundant in the matrix. They are finely crystallized and occur as small elongated needles or acicular rods. They are sometimes oriented and define the trachytic texture of the rock (Figure 5(c)). Clinopyroxene microlites are automorphic and less abundant (<2% by volume of the rock).

3.2.3. Phonolites

The phonolite lavas have a classic porphyritic microlitic texture (Figure 5(e)) with more or less hyalloclastic varieties. Alkali feldspar phenocrysts (1.5 × 0.8 mm and 15% - 20% by volume of the rock) are abundant in phonolites. They are automorphic, tabular. Other phenocrysts do not contain oxide inclusions but sometimes in the edges. The majority of phenocrysts have a cloudy, hazy appearance (Figure 5(f)). Clinopyroxene phenocrysts (1.3 × 0.8 mm, about 15% - 20% by volume of the rock) are automorphic. They are green and regularly corroded in the cores and sometimes in the rims by mesostasis. Clinopyroxene phenocrysts (1.3 × 0.8 mm, about 15% - 20% by volume of the rock) are automorphic. They are green and regularly corroded in the cores and sometimes in the rims by mesostasis. The iron-titanium oxide phenocrysts (1.2 × 0.9 mm, 5% - 10% by volume of the rock) are automorphic and very often corroded in the cores and rims.

The mesostasis of the phonolites consists mainly of alkali feldspar microlites, clinopyroxene and iron-titanium oxide microcrystals. The iron-titanium oxide microcrystals (less than 0.1 mm, about 10% by volume of the rock) are scattered in the matrix and sometimes included in clinopyroxene phenocrysts or fixed in the edges of alkali feldspar phenocrysts. They would come from the alteration and destabilisation of clinopyroxene phenocrysts. Alkali feldspar microlites (less than 0.1 mm) are the most abundant in the matrix (25% - 30% by volume of the rock). They are small acicular rods which show a preferential orientation in some places. They are mostly very finely crystallized. Clinopyroxene microlites are rare (1% to 3% by volume of the rock).

3.3. Mineralogy

3.3.1. Olivine

Chemical analyses of olivine crystals in the basanites are presented in Table 1.

Table 1. Chemical analysis of olivine crystals in Beka basanites.

lava	basalte						
sample	NGV1	NGV2	NGV3	NGV4	NGV5	BD1	BD2
SiO_2	38.38	38.67	38.73	38.49	37.72	38.72	38.21
FeO	19.29	19.57	19.57	19.78	22.24	19.92	23.91
MnO	0.22	0.28	0.24	0.26	0.32	0.34	0.49
MgO	41.02	40.89	41.05	40.76	38.89	40.96	36.26
CaO	0.25	0.26	0.22	0.25	0.14	0.24	0.23
NiO	0.04	0.13	0.1	0.1	0.07	0.12	0.01
Total	99.21	99.79	99.92	99.62	99.38	100.31	99.11
Fa	21.1	21.4	21.3	21.6	24.6	21.7	27
Mg #	79.1	78.9	78.9	78.9	78.6	78.6	75.7
Si	0.991	0.996	0.995	0.993	0.989	0.993	1.015
Fe^{2+}	0.417	0.421	0.42	0.427	0.487	0.427	0.531
Mn	0.005	0.006	0.005	0.006	0.007	0.007	0.011
Mg	1.579	1.569	1.572	1.568	1.519	1.566	1.436
Ca	0.007	0.007	0.006	0.007	0.004	0.007	0.006
Ni	0.001	0.003	0.002	0.002	0.001	0.003	0
Fo	78.9	78.6	78.7	78.4	75.4	78.3	73

The forsterite content of the phenocrysts in the Ngao Voglar basanites varies very little (78.4% to 78.9%). The Fo content of the olivine microcrystals shows a zonation with high contents in the core (Fo 78.9%) compared to the edges (Fo 75.4%). The lowest contents are found in the microcrystals of the mesostasis (Fo 73.0%). NiO contents are below 0.2 wt% and the lowest contents are found in basanites that outcrop as flows. CaO contents are high and range from 0.1 to 0.3 wt.% of oxides. Such high CaO contents characterize the olivines of alkaline lavas (Roeder & Emsly, 1970). They are different and high compared to those found in the spinel lherzolites of the mantle under Adamawa (Nkouandou & Temdjim, 2011) and some volcanic centers of the Cameroon Volcanic Line (Temdjim, 2012).

3.3.2. Clinopyroxene

The chemical compositions of clinopyroxene crystals from the basanites (flows and Voglar massif) of the Beka region are presented in **Table 2** and illustrated in **Figure 6(a)**. The nomenclature used to designate them is that of the classification of Morimoto et al. (1988). Clinopyroxene crystals are generally diopside in phenocrysts (Wo47-En49-Fs5) and microlites (Wo46-En39-Fs14). CaO contents decrease and FeO contents increase from phenocrysts to microlites. TiO_2 contents are high and range from 2.44 to 3.17 wt% of oxides. Al_2O_3 contents are also

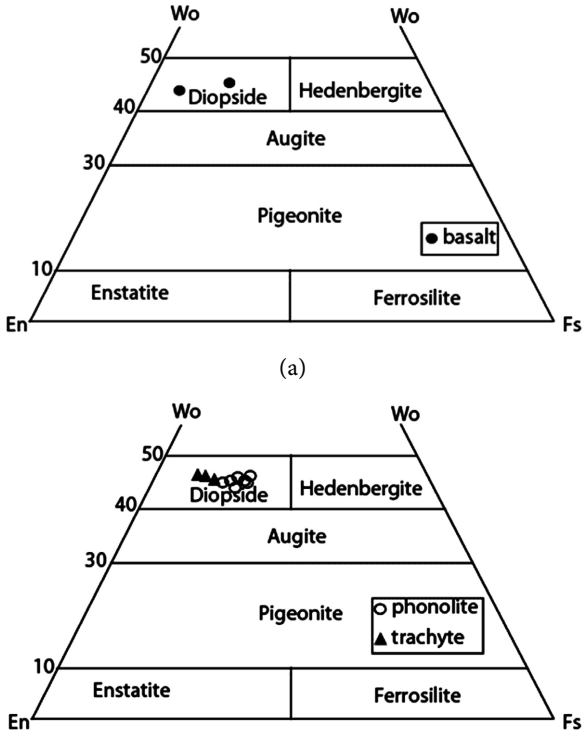

Figure 6. (a) Chemical composition of clinopyroxene crystals in basanites; (b) Composition of clinopyroxene crystals in felsic lavas in a Wo-En-Fs triangular diagram.

Table 2. Chemical analyses of clinopyroxene crystals in basanite lava.

lava	basanite		total	99.5	99.81
sample	NGV1	BD1	Si	1.739	1.717
SiO_2	46.31	45.3	Ti	0.069	0.09
TiO_2	2.44	3.17	Al	0.287	0.35
Al_2O_3	6.49	7.81	Cr	0.003	-
Cr_2O_3	0.1	0	Fe^{3+}	0.136	0.14
FeO	7.68	10.65	Fe^{2+}	0.105	0.198
Mno	0.18	0.46	Mn	0.006	0.015
MgO	13.04	9.5	Mg	0.73	0.537
CaO	21.93	20.99	Ca	0.882	0.852
NiO	0	0	Na	0.043	0.103
Na_2O	0.58	1.4	Wo	46	47
total	99.11	99.32	En	49	39
Fe_2O_3	4.82	4.9	Fs	5	14
FeO	3.35	0.24			

high and increase from the phenocrysts to the microlites (6.49% to 7.87%) as do Na_2O contents which range from 0.58% in the phenocrysts to 1.4% in the microlites.

In felsic lavas, i.e. trachytes and phonolites (Table 3), clinopyroxene crystals have a diopside composition (Figure 6(b)) The TiO_2 content of clinopyroxenes in all lavas varies from 0.53% to 2.48%.

The highest values are found in the clinopyroxene crystals of phonolites. Al_2O_3 contents reach 8.60% in phonolites compared to trachytes where they are between 2% and 2.38% by weight of oxides. The Na_2O content is high, ranging from 1.6% to 2.81% in the phonolites and compared to the content of the same oxide in the trachytes, which ranges from 1.5% to 1.8% by weight of oxides.

Some crystals have a high ZrO_2 content of 0.22%. The presence of cationic Al and Ti is assumed in the tetrahedral sites which contain less than 2% Si of the structural formula. The FeO content of clinopyroxene crystals increases slightly from the trachytes to the phonolite lavas. This increase is reflected in the ferrosilite contents which vary from 6% to 15% in the trachytes and from 10.7% to 19.4% in the phonolites (Table 3). The values of the Al^{VI}/Al^{IV} ratios are low and below 0.25.

3.3.3. Plagioclase

The compositions of the plagioclase microlites in the basanites of the Beka area are presented in Table 4 and shown in Figure 7. These plagioclase crystals are calcic and generally have a labrador composition (An 59.4 - 62.1, Ab 37.7 - 39.2, Or 1.3 - 1.7) in the lavas sampled on the Voglar massif and is (An 61.9 - 63.5, Ab 35.3 - 37.1, Or 1.1 - 1.5) in the surrounding flows. BaO contents are generally very low and vary between 0.03% and 0.11% in the lavas, 0.11% in the basanite lavas and flows of Beka. Cationic Al and FeO_3 contents are assumed in tetrahedral sites so Si contents are less than 3% of the structural formula.

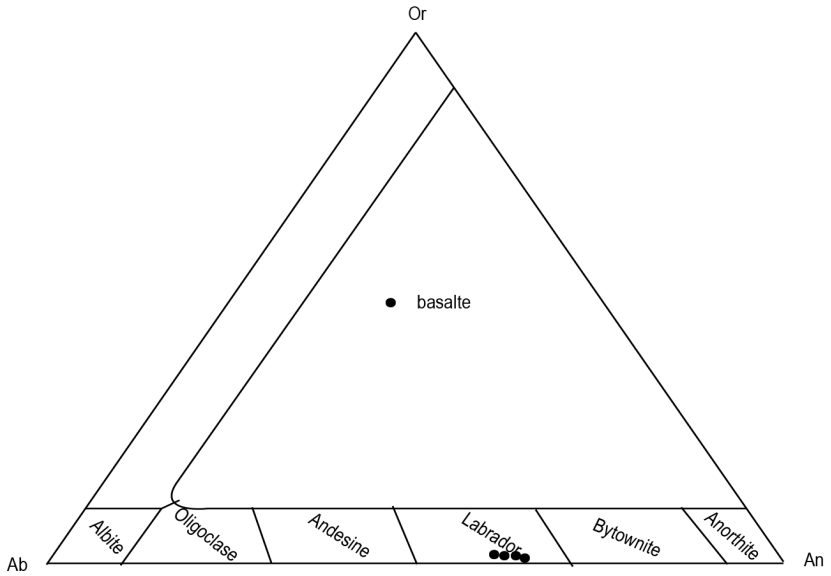

Figure 7. Plagioclase crystal composition of basaltic lavas in the Or-Ab-An.

Table 3. Chemical analyses of clinopyroxenes in felsic lavas.

lava	trachyte						phonolite					
sample	NG01	NG02	NG03	NGZ1	NGZ2	NGZ3	NGDF	NGDF	NGDF	NGB	NGB	NGB
SiO_2	49.08	49.7	48.73	43.37	46.51	47.71	47.83	50.25	49.6	47.67	48.92	50.39
TiO_2	1.1	1.19	0.99	2.48	1.7	0.94	1	0.56	0.53	1.77	1.28	0.93
Al_2O_3	2.22	2.38	2.07	8.62	6.42	4.4	4.23	2.22	3.31	5.88	4	1.78
FeO	11.44	10.94	11.55	13.78	11.96	14.92	13.98	13.78	14.4	12.38	12.77	14.5
FnO	1.54	1.6	1.58	0.73	8.63	1.28	1.47	2.37	1.77	0.83	1.25	2.05
MgO	10.75	10.58	10.63	7.54	9.2	7.58	8.13	8.45	8.15	8.94	9.17	8.15
CaO	21.04	21.52	21.02	21.37	21.36	20.41	19.91	19.95	19.08	20.9	20.95	20.3
Na_2O	1.57	1.52	1.67	1.62	1.57	1.63	2.5	2.14	2.81	1.79	1.81	2.33
ZrO_2	0.21	0.14	0.21	0.22	0.03	0.15	-	-	-	0.1	0.06	0.08
Total	98.97	99.57	98.45	99.73	99.38	99.41	99.19	99.94	99.85	100.24	100.2	100.5
Fe_2O_3 (cal)	7.57	7.72	8.46	9.72	7.21	6.7	9.97	6.82	9.33	6.24	6.65	7.55
FeO (Cal)	4.63	5.4	3.94	5.03	5.47	8.89	5.01	7.65	6	6.77	6.78	7.71
Total (Cal)	99.73	101.3	99.3	100.7	100.11	100.09	100.19	100.62	100.78	100.86	100.87	101.26
Si	1.867	1.865	1.863	1.653	1.763	1.835	1.824	1.913	1.879	1.796	1.846	1.91
Ti	0.031	0.034	0.028	0.071	0.049	0.027	0.029	0.016	0.015	0.05	0.036	0.026
Al VI	-	-	-	0.04	0.049	0.034	0.015	0.013	0.027	0.056	0.024	0
Al IV	0.1	0.105	0.093	0.347	0.237	0.165	0.176	0.087	0.121	0.204	0.154	0.079
Fe (+3) VI	0.183	0.175	0.199	0.279	0.206	0.194	0.286	0.195	0.266	0.177	0.189	0.205
Fe^{2+}	0.147	0.17	0.126	0.16	0.173	0.286	-	-	-	0.213	0.214	0.24
Mn	0.05	0.051	0.051	0.024	0.02	0.042	0.047	0.077	0.057	0.026	0.04	0.066
Mg	0.61	0.592	0.606	0.042	0.52	0.434	0.462	0.48	0.461	0.502	0.516	0.46
Ca	0.857	0.865	0.861	0.873	0.867	0.857	0.814	0.814	0.774	0.843	0.847	0.825
Na	0.117	0.111	0.124	0.12	0.115	0.121	0.185	0.158	0.206	0.13	0.133	0.171
Zr	0.004	0.003	0.004	-	-	-	-	-	-	0.002	0.001	0.002
WO	49.2	49.2	50.1	51.2	49.5	49.2	51	48.3	49.1	48.5	49.1	50.1
En	42.3	40.8	43.1	38.1	39.1	31.4	38	34.7	36.9	36.7	36.7	33.1
Fs	8.5	10	6.8	10.7	11.3	19.4	11.1	16.9	14	14.8	14.2	16.8

Table 4. Chemical analyses of plagioclase crystals in basaltic lavas.

	Lava basaltes								
sample	NGV1	NGV2	NGV3	NGV4	NGV5	BD1	BD2	BD3	BD4
SiO_2 (% pds)	52.38	52.81	52.54	51.94	52.21	52.05	52.16	51.39	51.94
Al_2O_3	30.07	27.95	29.27	29.24	30.13	29.05	29.54	29.12	30.25

Continued

CaO	12.03	11.66	12.23	12.18	12.39	12.18	12.27	12.57	12.54
Na_2O	4.24	4.42	4.17	4.11	3.98	4.02	3.97	3.85	4.02
K_2O	0.22	0.23	0.23	0.24	0.28	0.17	0.25	0.19	0.2
BaO	0.11	0.03	-	0.05	0.16	-	0.02	0.12	-
total	99.05	97.1	98.44	97.76	99.15	97.49	98.19	97.24	98.95
Si (apuf)	2.39	2.45	2.41	2.39	2.38	2.41	2.4	2.39	2.37
Al	1.61	1.53	1.58	1.58	1.62	1.58	1.6	1.59	1.63
Ca	0.59	0.58	0.6	0.6	0.61	0.6	0.6	0.63	0.61
Na	0.38	0.4	0.37	0.37	0.35	0.36	0.35	0.35	0.36
k	0.01	0.01	0.01	0.01	0.02	0.01	0.02	0.01	0.01
Ba	-	-	-	-	0.16	0.02	-	0.12	-
Or (% pds)	1.5	1.4	1.3	1.5	1.7	1	1.5	1.1	1.2
Ab	37.7	39.2	36.5	36.5	36.2	37.1	36.4	35.3	35.6
An	60.9	59.4	61.7	62	62.1	61.9	62.1	63.5	63.2

3.3.4. Alkali Feldspars

Chemical analyses of alkali feldspar crystals from felsic lavas are presented in Table 5. They have a composition of anorthose (Ab 54.0 - 72.4 Or 23.7 - 44.4 An 1.8 - 3.9) as shown in Figure 8. Some phenocrysts analyzed in phonolites have a composition that is close to that of sanidine (Or 56.6-Ab 40.6-An 2.7). Another analysis found in feldspar crystals of phonolites is that of oligoclase (Ab 40.6 Or 56.6 An 2.7) with anorthite content of 12.4%. anorthite content of 12.4%. The other compositions are: anorthose (Ab 54.0 Or 44.4 An 1.8), oligoclase (Ab 70.4 Or 18.4 An 11.2), and andesine (Ab 65.5 - 66.6 Or 9.7 - 10.4 An 23.7 - 24.2). FeO contents are relatively high in the trachytes (0.49%) compared to the phonolites (0.32%). Some anorthose crystals of the phonolites have high BaO contents (up to 2.84% by weight of oxides).

3.3.5. Iron Titanium Oxides

1) Titanomagnetites

Representative chemical analyses and structural formulae of titanomagnetite crystals are presented in Table 6. For basanite lavas, the composition of titanomagnetite is characterized by high TiO_2 contents of 20% to 23% by weight of oxides. Their FeO content is between 60% and 67% by weight of oxide. MgO contents are between 3% to 4% by weight of oxides to when the MnO content is low (strictly less than 1% by weight of oxide). Their Al_2O_3 contents are between 1% and 3% by weight of oxide. All these compositions are different and sometimes very high compared to those of the Titanomagnetites of the differentiated lavas (Table 7). In the latter, the TiO_2 contents are low and range from 7% to 11% by weight of oxides, their FeO contents are low compared to those of basanite.

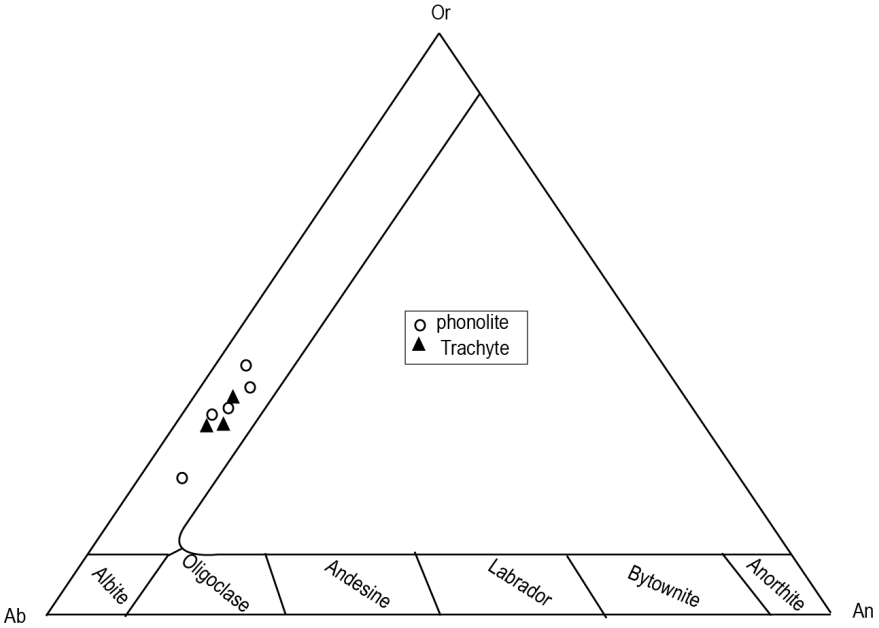

Figure 8. Alkali feldspar crystal composition of felsic lavas.

Table 5. Chemical analysis of alkali feldspar crystals in felsic lavas.

	Lava trachyte phonolite										
sample	NGO1	NGO2	NGO3	NGZ1	NGZ2	NGDF1	NGDF2	NGZ1	NGZ2	PD1	PD2
SiO_2	64.34	65.77	65.51	66.32	63.21	66.32	63.21	66.29	62.48	66.35	61.93
Al_2O_3	19.97	19.87	20.11	19.71	20.28	19.71	0.28	19.47	20.58	20.30	22.60
FeO	0.32	0.49	0.41	-	-	0.17	0.16	0.18	0.32	0.16	0.21
CaO	0.57	0.62	0.73	0.45	0.83	0.45	0.83	0.37	0.85	0.74	2.76
Na_2O	6.81	7.71	7.43	7.47	8.47	7.46	8.41	6.26	6.44	7.07	8.61
K_2O	6.61	6.02	6.05	6.42	4.22	6.42	4.22	7.81	6.08	6.44	3.31
BaO	1.42	0.15	0.22	-	0.06	-	0.06	0.00	2.84	0.47	1.09
Total	99.62	100.56	100.51	100.35	97.084	100.53	97.283	100.38	99.59	101.52	100.49
Si	2.928	2.935	2.926	2.959	21.904	2.960	2.900	2.968	2.874	2.937	2.784
Al	1.071	1.045	1.051	1.036	1.094	1.040	1.100	1.027	1.116	1. 059	1.198
Fe^{2+}	0.012	0.018	0.015	-	-	0.010	0.010	0.007	0.012	0.006	0.08
Ca	0.028	0.030	0.035	0.022	0.041	0.020	0.040	0.018	0.042	0.035	0.133
Na	0.608	0.669	0.645	0.647	0.759	0.650	0.760	0.545	0.576	0.608	0.752
K	0.384	0.343	0.345	0.366	0.247	0.370	0.250	0.446	0.357	0.363	0.19
Ba	0.025	0.003	0.004	0.000	0.001	-	-	0.000	0.051	0.008	0.019
Or	37.8	33.1	33.9	35.3	23.7	35.3	23.7	44.4	39.8	57.6	17.6
Ab	59.4	64.1	62.7	62.6	72.4	62.6	72.4	54.0	56.1	40.6	70.0
An	2.7	2.8	3.5	2.1	3.9	2.1	3.9	1.8	4.1	2.7	12.4

Table 6. Chemical analysis of Titanomagnetites and ilmenite from basalts.

lava	basalte		ilménite	
sample	NGV1	NGV2	BD1	BD2
SiO_2	0.09	0.94	0.08	0.16
TiO_2	22.36	21.13	21.89	43.52
Al_2O_3	1.78	2.68	1.75	0.65
Cr_2O_3	0.54	0.23	0.12	0.04
Fe_2O_3	-	-	-	-
FeO	66.19	65.37	67.79	49.81
MnO	0.98	0.94	0.9	0.97
MgO	3.8	4.01	3.54	3.46
CaO	0.27	0.23	0.07	0.07
NiO	0.04			0.05
Total	86.06	96.3	96.15	98.74
Fe_2O_3 Cal	-	-	-	19.75
FeO Cal	-	-	-	32.04
Total Cal	-	-	-	100.72
Si	0.026	0.272	0.024	0.01
Ti	4.912	4.768	4.813	1.61
Al	0.614	0.911	0.603	0.04
Cr	0.125	0.052	0.069	-
Fe^{3+}	0.218	4.793	5.527	0.73
Fe^{2+}	10.947	11.001	11.047	1.32
Mn	0.243	0.231	0.224	0.04
Mg	1.653	1.727	1.545	0.25
Ca	0.085	0.073	0.022	-
Ni	0.01	-	-	-
Mol %	62.92	64.51	61.49	-

Table 7. Chemical analysis of Titanomagnetite in felsic lavas.

	lava trachyte phonolite					
sample	NGZ1	GZ2	NGDF1	NGDF2	NGB1	NGO1
TiO_2	9.97	9.59	8.36	10.64	7.78	10.32
Al_2O_3	0.72	0.51	0.13	0.12	0.55	0.53
Cr_2O_3	0.2	0.02	0.02	0.02	-	0.01
Fe_2O_3	48.39	49.27	50.62	48.41	53.27	43.51
FeO	35	34.58	33.09	33.89	33.65	32.43
MnO	4.19	4.47	5.05	6.94	4.09	5.6

Continued

MgO	0.6	0.44	0.03	0.16	0.33	0.3
total	98.88	98.97	97.59	100.17	99.68	92.7
Ti	0.125	0.12	0.105	0.133	0.097	0.129
Al	0.014	0.012	0.003	0.002	0.011	0.01
Cr	-	-	-	-	-	-
Fe^{2+}	1.091	1.096	1.092	1.076	1.133	0.994
Mn	0.059	0.063	0.071	0.098	0.058	0.079
Mg	0.015	0.011	0.001	0.004	0.008	0.007
Mol %	26.79	25.6	22.29	26.63	20.63	28.86

of oxides, their FeO content is low compared to that of basalts and ranges between 32% and 35% by weight. 35% by weight. MgO contents are low (strictly less than 1% by weight) when MnO contents are high, between 4% and 7% by weight of oxide. Their molar contents in United States Pharmacopoeia (USP) are low compared to the Titanomagnetites of basanite lavas which are between 20% and 29% by weight of oxide.

2) Ilmenite

The chemical analysis and structural formula of the ilmenite crystal is presented in Table 6. The TiO_2 content is 43.52% by weight and the FeO content is 49.89% by weight. This composition is characterised by the high MgO content (3.46 wt% oxide) and low in Cr_2O_3 content (0.04% by weight of oxide) and that of MnO (strictly less than 1% by weight of oxide). The temperatures calculated from the empirical calibration of Sthomer, (1983) on the basis of the coexistence of ilmenite and titanomagnetite in basanites are 376% ± 50% ˚C. basanites are 376% ± 50% ˚C. The oxygen fugacity is high (Fo_2 = 10 - 5.7 atm) (Figure 9).

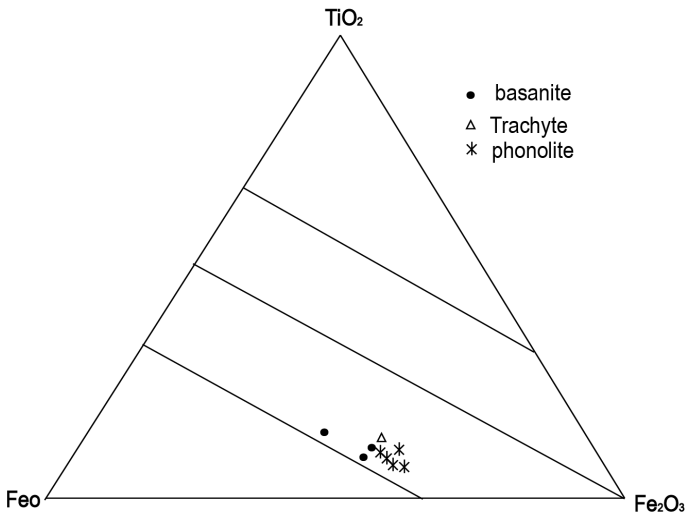

Figure 9. Composition of Fe-Ti oxide crystals in the TiO_2-FeO-Fe_2O_3 diagram.

3.4. Geochemistry

3.4.1. Major Element Variations

The geochemical compositions of the analyzed rocks are presented in **Table 8** are used for classification, petrogenetic and geotectonic investigations. According to the TAS (Total Alkali vs Silica) diagram (Le Bas et al. 1986), the studied have compositions of basanite, trachyte and phonolite respectively. Basanite have SiO_2 contents of 41.66 wt% characteristic of ultrabasic lavas (SiO_2 < 45%). The phonolites have SiO_2 contents ranging from 56 - 58 wt%, lower than those of the Kapsiki plateau (SiO_2: 59.4%) (Ngounouno et al., 2006). TiO_2 contents are high in the Beka basanites (4.5 wt%) compared to those of Mt. Cameroon (3.5 wt%) (Wandji et al., 2009). They are significantly low in the differentiated lavas of the Beka region (0.48 - 0.63 wt%) and the Cameroon Volcanic Line (strictly less than 1%). Al_2O_3 contents are low in the volcanic formations (less than 15%) compared to the differentiated lavas of the two volcanic centres (between 15% and 21% by weight). In contrast, Fe_2O_3 content is high in the basanites (13.91% - 14.23%) and low in the differentiated formations of Beka (between 2% and 4%) and the Cameroon Volcanic Ligne (3% and 8% by weight) (Marzoli et al., 1999; Ngounouno et al., 2006). The MnO contents are strictly below 0.3% in all volcanic formations. The MgO contents are high in the volcanic formations (6 and 10 wt%). The highest value (9.28%) is found in the basanites of Mt. Cameroon. The same variations are observed for CaO contents ranging from 10.20% in the Beka and Mt. Cameroon basanites (11.18% by weight All the analyzed samples, likewise those from the Kapsiki Plateau (Ngounouno et al., 2000), Mt Cameroon (Wandji et al., 2009), Mt Bamenda (Kamgang et al., 2010) and the volcanic island of Sao Tome (Marzoli et al., 1999) plotted for comparison evidence alkaline affinities (**Figure 10**).

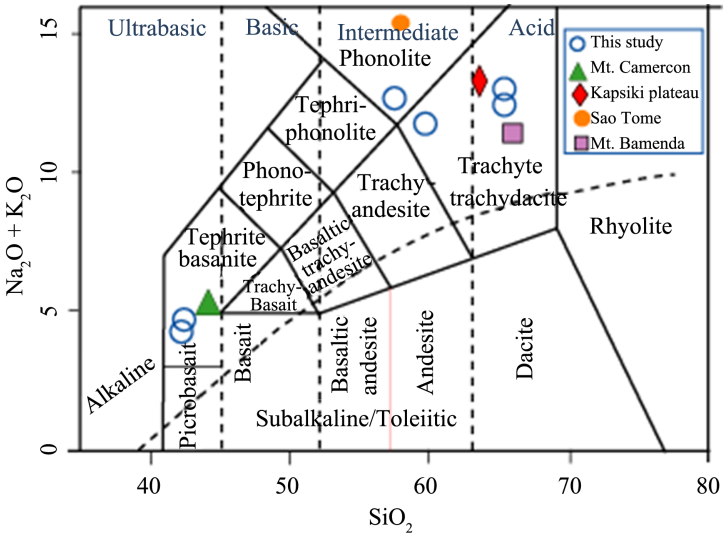

Figure 10. Distribution of the sum of alkalis from the Beka volcanism as a function of silica. Analyses of the Kapsiki Plateau (Ngounouno et al., 2000), Mt. Cameroon, (Wandji et al., 2009), Mt. Bamenda (Kamgang et al., 2010) and Sao Tome (Marzoli et al., 1999) are added for comparison.

Table 8. Chemical analyses and CIPW standards of lava from the Beka area.

sample	NGV1	NGV2	NGO1	NGO2	NGDF1	NGDF2	MTC	PK	ST	MTB
SiO_2	41.66	41.91	60.66	60.87	57.99	56.37	43.04	59.4	61.68	60.36
TiO_2	4.5	4.8	0.49	0.47	0.63	0.65	3.23	0.6	0.65	0.39
Al_2O_3	14.51	14.59	19.21	19.19	18.9	20.16	13.57	18.31	18.26	15.13
Fe_2O_3	14.23	14.33	2.95	2.93	3.59	3.24	13.91	5.65	3.73	7.36
MnO	0.2	0.2	0.2	0.19	0.24	0.23	0.21	0.2	0.21	0.21
MgO	6.52	6.57	0.23	0.2	0.75	0.25	9.28	0.14	0.31	0.04
CaO	10.1	10.25	2.02	2.03	2.68	3.14	11.18	1.18	1.25	2.51
Na_2O	3.55	3.81	5.79	5.77	0.3	5.8	3.41	7.75	10.09	5.72
K_2O	0.92	0.93	5.82	5.8	5.45	5.09	1.43	4.69	5.49	5.19
P_2O_5	0.84	0.87	0.3	0.19	0.17	0.3	0.75	0.11	0.08	0.09
LOI	1.78	1.88	1.93	1.98	2.07	4.05	-	1.87	1.96	2.55
total	98.81	100.14	99.6	99.62	92.77	99.28	100.01	99.9	103.71	99.55
Be (ppm)	1.5	1.9	-	93	4.9	-	2.055	7	0.3	0.3
Rb	45.15	45.19	203	204	148	138	39.16	165	175	5.89
Sr	969.1	967.1	377	375	604	1923	1078	249	177	66
Cs	0.43	0.437	1.55	1.6	0.98	1.2	0.492		3.61	35
Ba	564.5	563.5	1150	1152	840	-	-	781	2.67	0.4
V	321	319	25	23	17	29	287.4	-	0.9	940
Cr	25.52	26.2	7	4.7	-	8	326.3	18	3.1	0.22
Co	43.12	42.12	5	1.8	1.6	6	50.75	-	1	2.55
Ni	23.6	23.42	7	2	-	5	159.4	8	2.7	0.22
Cu	31.38	31.39	178	180	-	9	67.36	9	-	1.61
Zn	157.3	158.9	-	244	15	-	130.4	257	156.8	-
Y	32.05	32.07	-	74.4	39.2	-	31.58	37	35.3	-
Zr	435	435	956	955	1021	812	427	1055	1088	48
Nb	86.88	86.91	227.2	228	180	4.41	116.496	178	216.6	682
Hf	9.295	9.292	18	19	20.5	18	9.003	6.6	21.06	97
Ta	1.774	5.858	22.7	15	6.7	12.3	7.281	17.06	15.69	15
U	6.118	6.118	14.2	23	21.56	23.9	8.586	22.5	24.9	6.89
Th	5.858	1.774	3.96	3.88	12.33	196.8	-	23.8	6.8	10
La	53.09	53.06	131.7	131.9	139.5	-	84.61	135.5	163.1	97
Ce	114.3	114.08	186	187	240	84.61	173.6	224	254.9	201
Pr	12.85	12.82	-	39.5	23	173.6	20.01	-	24.2	24

Continued

Nd	55.84	55.83	-	132	74	20.01	75.65	75.4	72.9	97
Sm	0.336	1.137	8.2	8.3	10.9	0.339	12.97	12.4	10.37	17.3
EU	3.567	3.564	2.88	2.89	2.96	12.97	3.91	3	2.07	5.94
Gd	9.65	9.67	0.96	14.25	8.07	3.91	9.895	9.6	7.92	13.58
Tb	1.312	1.314	-	0.98	1.218	9.895	1.327	-	1.16	1.87
Dy	6.872	6.876	-	12.5	0.62	1.327	6.885	7.2	6.28	10.23
Ho	1.157	1.155	-	2.42	1.3	6.885	2.311	-	1.16	1.97
Er	2.904	2.906	-	7.01	3.77	1.142	2.86	4	0.51	4.65
Tm	0.365	0.368	-	1.06	0.57	2.86	-	-	0.49	0.7
Yb	2.27	2.29	4.03	4.05	3.93	2.311	0.339	0.46	3.32	4.3
Lu	11.37	0.336	-	1.09	6.95	75.65	1.142	2.76	3.29	0.69

3.4.2. Trace Elements

The trace elements compositional variations of the studied lavas are presented in Table 8. The transition elements have very low contents. Ni, Co and Cr range from 23.6 - 23.42 ppm; 43.12 - 42.12 ppm and 25.42 - 26.2 ppm respectively in the basalts and present lower values in the differentiated lavas.

In Figures 11(a)-(h), the binary diagrams of Ba, Nd, La, Rb and Zr versus silica do not show clear positive correlations in the lavas studied, indicating generally incompatible behavior throughout the series. Cr and Ni contentsare very low (<30 ppm) within all the studied samples, compared to the lavas of the Kapsiki Plateau in the Far North of Cameroon, with concentrations up to 326.3 ppm and 159.4 ppm respectively.

The elements Co, Sc, V, Cu, indicate positive correlations in the evolved terms, contrary to the basanite lavas where we rather observe negative correlations meaning compatible behaviours, their concentration decreases according to the evolution of the silica content Table 8. These same variations are observed in the Kapsiki Plateau, Mt Cameroon and Sao Tome Island volcanic lavas. Co, Sc, V, Cu, although not represented in this diagram, indicate positive correlations in the evolved terms, contrary to the basanite lavas where negative correlations are rather observed meaning compatible behaviours, their concentration decreases according to the evolution of the silica content Table 8. These same variations are observed in the lava of the Kapsiki Plateau, Mt Cameroon and the volcanism of Sao Tomé Island.

The Beka basanites like those of Mt. Cameroon are characterized by very strong negative anomalies in K and slight negative anomalies in P and Ti. Slight positive anomalies are observed in Nb, Ta, Sr and Eu in the Beka basanites. The Beka basanite spectrum is similar to those of the Cameroon Line. They show very strong negative anomalies in K, P and Ti. Positive anomalies are observed in Nb, Ta, Hf and Zr. Nb/Ta ratios are relatively constant (between 14 and 16) in all the Beka volcanic rocks (Figure 12).

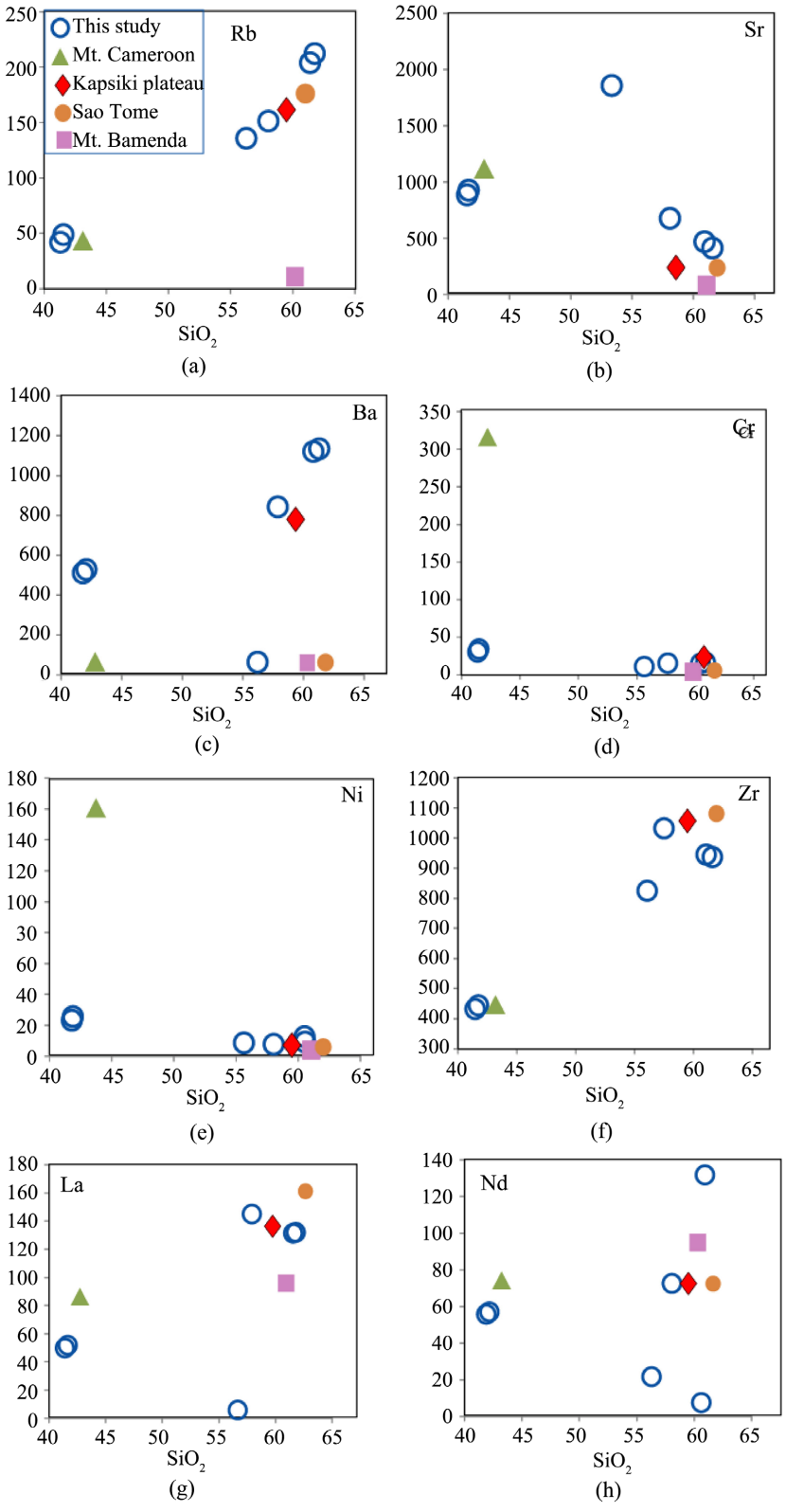

Figure 11. Variation of some trace elements (ppm) as a function of SiO_2 (wt %). Data from the Kapsiki Plateau (Ngounouno et al., 2000), Mt. Cameroon (Wandji et al., 2009), Sao Tome (Marzoli et al., 1999) and Mt. Bamenda (Kamgang et al., 2010) are shown for comparison.

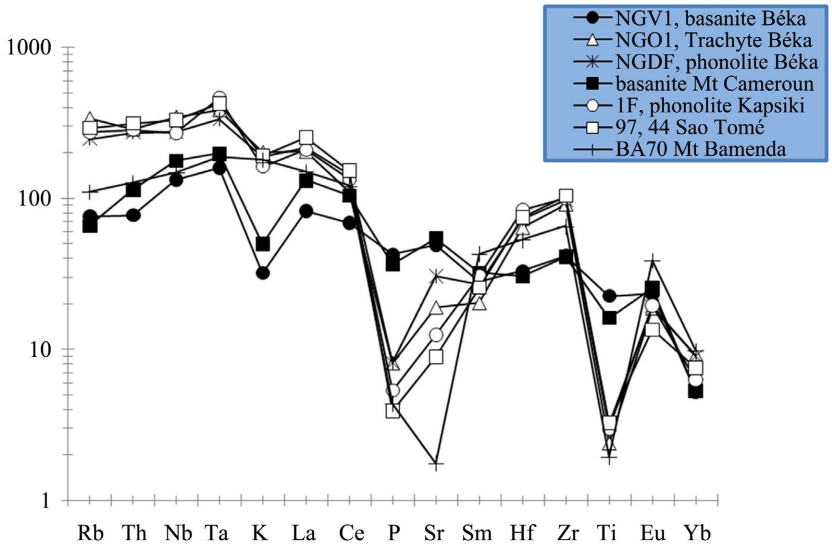

Figure 12. Multi-element patterns of trace element analyses from Beka volcanism normalized to the primitive mantle (McDonough & Sun, 1995). Those from Mt. Cameroon and Sao Tome are shown for comparison.

The rare earth spectra normalised to the primitive mantle of (McDonough & Sun, 1995) are shown in **Figure 13**. They are steep and are characterized by High Light Rare earth contents that reach 90 to 300 times the mantle values anomalies are observed in all basanites and differentiated lavas except for the Eu anomaly in the Sao Tomé phonolite.

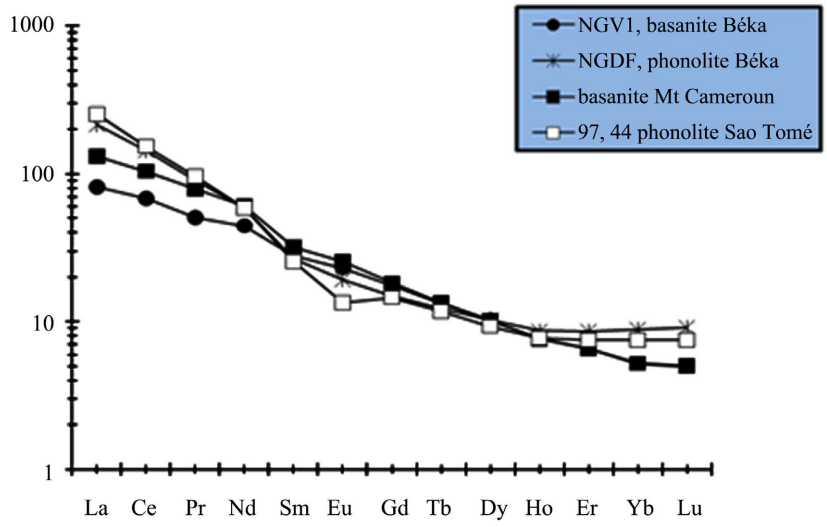

Figure 13. primitive mantle normalized REE diagram of the Beka volcanic rocks (McDonough & Sun, 1995). Those from Mt. Cameroon and Sao Tomé are shown for comparison.

4. Discussion

4.1. Development of Beka Volcanism and Magmatic Evolution

The present work shows that the Beka volcanism developed a series of forma-

tions consisting of domes sensu stricto, conical domes and dome flows characterised by basanites, trachytes and phonolites. The study of the different processes and mechanisms that led to magmatic differentiation and petrographic diversity will give us an idea of the different petrogenetic processes involved in the formation of these rocks. These processes and mechanisms are generally characterised by fractional crystallisation, partial melting, magma mixing or crustal contamination. In the course of the discussion, the lavas of Beka and its surroundings are compared with those of other volcanic formations of the Cameroon Volcanic Line such as the lavas of Mount Cameroon, Mt Bamenda, and the Kapsiki Plateau and Sao Tomé. The latter, studied by several authors, are of mantle origin and result from weak partial melting of a deep asthenospheric mantle (Déruelle et al., 2000; Ngounouno et al., 2000; Marzoli et al., 1999; Ngounouno et al., 2006; Wandji et al., 2009; Kamgang et al., 2010, Tchop et al., 2020).

The mineralogical study of the lavas of the Beka region reveals the evolution of the chemical compositions of microlite phenocrysts from relatively primitive lavas (basanite) to differentiated lavas. Fo contents decrease from phenocrysts (Fo 79%) to microlites (Fo 75%). (Fo 75%). Iron contents increase relatively from clinopyroxenes in basanites to those in felsic lavas. The TiO_2 and MgO contents of the iron-titanium oxides decrease from the basanites to the phonoliths, contrary to those of Fe and Mn. All these changes may reflect the differentiation of the parent magma in the series the driving force behind this differentiation would be the process of fractional crystallisation.

This hypothesis is supported petrographically by the presence of basanite enclaves in the trachytes, which suggest the origin of all the lavas in the same mantle environment.

The low values of the Al^{VI}/Al^{IV} ratios of clinopyroxene crystals in the Beka lavas (less than 0.25) suggest the equilibrium pressures of suggest the relatively low equilibrium pressures of crystallization (Wass, 1979). The TiO_2 content of clinopyroxene crystals is high (3.17 wt%) indicating low crystallization temperature (Ferguson, 1977) and a low oxygen fugacity during crystallization (Nielsen, 1979). The mineralogical composition of the Beka volcanism is similar to that of lavas reported in other volcanic environments of the Adamawa plateau (Nono et al., 1994; Nkouandou et al., 2010; Temdjim et al., 2004) and the enttire CVL (e.g Kamgang et al., 2008; Wandji et al., 2009; Marzoli et al., 1999).

4.1.1. Laying of the Lavas

Beka domes are roughly conical in shape and strongly prismatic (**Figure 3(a)**). The conical shape and prismatic structure observed in lava outcrops are generally due to the cross-fracture emplacement and cooling process of highly viscous lavas, respectively. A similar mechanism has been proposed to explain the morphology and prismatic structure of the Atakor volcanic edifices (Girod, 1968). According to this mechanism, as the viscous magma rises, it begins to cool and thermal shrinkage cracks isolate polygonal prisms between them. These prisms,

pushed as if through spinnerets into vertical columns tightly packed together, curl into divergent sheaves at the surface. The dome-cast massifs (**Figure 3(b)**) would therefore result from their placement on an inclined surface (Girod, 1968). This consideration explains well the dome-cast shape of the trachytic massif, which is built on the sloping side of a small cliff. The conical shape of the phonolite massif can be explained by the fact that this massif was built at the intersection of fractures (**Figure 3(c)**).

4.1.2. Crustal Contamination

In the absence of isotopic analyses, the arguments presented for crustal contamination are speculative. The contamination of the Beka felsic and basaltic lavas is discussed here on the basis of their geochemical characteristics. The interaction of the magma with the rocks it passes through, during its magmatic ascent, such as basement rocks, can modify its composition. The influence of these traversed rocks can be detected through certain major element contents or trace element contents and ratios.

Contamination is sometimes suggested by the presence of basement enclaves and/or other rocks. The levels of major elements such as SiO_2 and TiO_2 can be used to determine whether contamination is present. The high TiO_2 (4.8% - 4.9%) and SiO_2 (41.57% - 41.91%) contents of basanites reflect their very negligible contamination. Their TiO_2 contents are similar to those of other uncontaminated lavas of the Cameroon Volcanic Line with a mantle origin similar to that of the OIBs (Arndt et al., 1993; Zhao et al., 1994; Ewart et al., 1998, 2004).

In general, the behaviour of certain trace elements, such as Sr, Zr, Ta and Nb are used to attest the involvement of crustal contamination (Cai et al., 2010). Very often crustally contaminated mafic rocks show negative Nb and Zr and positive Sr anomalies on the multi-element diagram (Cai et al., 2010). Also high LREE values with flat HREE spectra indicate crustal contamination of mafic rocks. The rare earth and multi-element spectra of the Beka volcanism show respectively a steep slope and the absence of systematic negative anomalies in Nb and Ta. This leads us to believe that the Beka formations and its surroundings would have suffered no or very negligible contamination.

In the Rb/Y vs. Nb/Y digram in **Figure 14**, part of the Beka rocks as well as the Mount Cameroon, Kapsiki Plateau formations are positioned within the field of uncontaminated alkaline basalt and felsic rocks. These results are in agreement with those of (Ngounouno et al., 2000, Déruelle et al., 2000; Tchop et al., 2020). A second part of the Beka and Kapsiki Plateau rocks are located between the field of uncontaminated formations and the field of basement rocks defined by (Kamgang et al., 2010) called "felsic and Precambrian basement of the Bamenda Mountains". This second part remains close to the field of uncontaminated alkaline basaltic and felsic rocks. This leads us to conclude that the contamination was negligible and point to cryptic contamination.

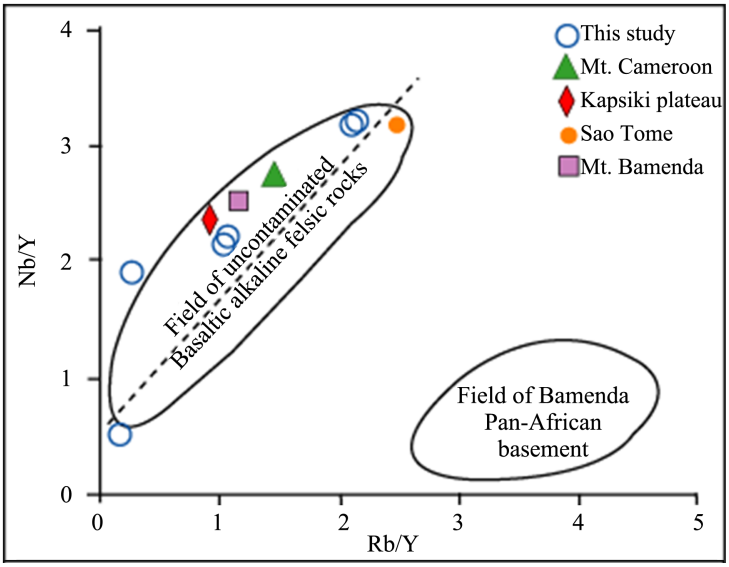

Figure 14. Basanite alkaline magmas are often enriched in Nb and then have relative low Rb/Nb. On contrary, crustal rocks and melts derived there from generally have higher Rb/Nb ratios (Weaver & Tarney, 1984). In Nb/Y vs Rb/Y plot, Cox & Hawkesworth (1985), show that melts could be separated into contaminated and uncontaminated The first one have higher Rb/Y ratios and low Nb/Y values, and the second ones are positively and steeper slope.

4.1.3. Fractional Crystallisation

Geochemical analyses of major, trace and rare earth elements show that SiO_2, Al_2O_3, Na_2O and K_2O contents are low in basalts compared to those of the same oxides in phonolites and trachytes. On the other hand, MgO, TiO_2, Fe_2O_3, CaO and to a lesser extent P_2O_5 contents are high in basalts compared to felsic lavas. The decrease in MgO, TiO_2, CaO and P_2O_5 contents reflects the crystallization of iron-titanium oxide, olivine and plagioclase in the basanites. The high contents of SiO_2, Na_2O, Al_2O_3 and K_2O in the differentiated lavas suggest the accumulation of alkali feldspar crystals in these rocks. Such a consideration is supported by the high values of alkali feldspar crystals in the differentiated lavas. The positive Zr and Hf anomalies could reflect the accumulation of feldspars in the Beka lavas and its surroundings.

Trace element data show that the transition element contents of the first series (Co, Ni, Cu and Zn) are very low compared to those of the primitive lavas which are directly derived from the partial melting of a mantle source (Green et al., 1973). Basanites have evolved through the crystallization of olivine crystals, plagioclase, and clinopyroxene, iron-titanium oxide crystals from an evolved parent magma. Such variations mark an evolution of the parent magma by the process of fractional crystallisation, as indicated in the other volcanic centers of the Cameroon Volcanic Line, for example the lavas of the Kapsiki Plateau, Mount Cameroon and Mt Bamenda.

4.1.4. Petrogenesis and Origin of Magmas

In the lavas presently studied, the rare earths normalized to the early mantle

(McDonough & Sun, 1995) are steeply dipping and characterized by high contents of light rare earths that reach 90 to 300 times the mantle values (**Figure 13**). These values indicate that the lava study is the result of a highly evolved mantle parent magma Toteu et al. (2004). The low values of heavy rare earth elements suggest the presence of garnet in the source of the Beka lavas. The rare earth element profiles of these lavas are tilted (**Figure 13**) and may indicate their derivation from a relatively low degree of partial melting from an enriched mantle source. The negative Eu anomalies indicate feldspar fractionation.

There is an increase in incompatible elements from Rb to Ta. These high incompatible element contents compared to the incompatible elements are an argument for a low partial melt rate of the source. Trace element spectra, normalised to the early mantle of (McDonough & Sun, 1995) of the Beka lavas and its surroundings in **Figure 12**, show correlations with each other. There is a parallelism with the trace element spectra of the Kapsiki plateaux, Mount Cameroon, Mt Bamenda and Sao Tome lavas. This would indicate a similarity in their geochemical characteristics.

In the compatible elements the contents progressively decrease attesting that the magma would have evolved with the fraction of a Cr and Ni rich mineral such as olivine or clinopyroxene. Magmas of intermediate or felsic composition have two main formation processes which are fractional crystallisation and assimilation. They can also be formed by the interaction of felsic and contemporary mafic magmas as suggested by Tchop et al. (2020); or partial melting of crustal material (Nkouandou et al., 2008; Ngwa et al., 2019), or partial melting of the metasomatised mantle wedge. The absence of mafic enclaves or mafic-felsic mixtures in the study area excludes the hypothesis of interaction of felsic and contemporary mafic magmas.

5. Conclusion

New petrographical and mineralogical data in relation with the magmatism of the Beka volcanic massifs situated at the Ngaoundere Plateau, in the northeastern part of the CVL, consists of alkaline basalts and basanites capped by trachytes and phonolitic flows. The most recent volcanism in this area consists of cinder cones aligned in a WNW-ESE direction, sometimes producing small lava flows. They are dominantly monogenetic and alternate with more evolved polygenetic volcanoes (e.g. Kapsiki plateau, Mts Bamenda).

In details, the Beka volcanism consists of basanite, trachyte and phonolite domes. The shape of the outcrops was acquired during their cooling and according to the topography. The lavas belong to the same magmatic series of an alkaline signature. The basanites have microlitic porphyrytic textures and consist of olivine, diopside, and titanomagnetite crystals. The felsic lavas have generally trachytic textures and are composed of anorthose, sanidine, oligoclase and andesine, slightly iron-rich diopside and titanomagnetite. All the lavas are nepheline normative and originate from depleted mantle source. The lavas belong to the same magmatic series, and show an alkaline and probably uncontaminated na-

ture. They evolved by fractional crystallization after partial melting. The geochemical characteristics point that these lavas would come from a low melting rate from an enriched mantle source. The felsic lavas are thought to have evolved by fractional crystallization of basanite magma. All these lavas present geochemical characteristics close to those of other regions of the Cameroon Volcanic Line.

These first data on the magmatism of Beka, allowed us to present preliminary results on the zone. Several other data are being collected for a better geochemical, isotopic and geochronological characterization of these formations.

Acknowledgements

We sincerely thank Prof Nkouandou Oumarou Faarouk for his support by providing chemical analyses.

Conflicts of Interest

The authors declare no conflicts of interest regarding the publication of this paper.

References

Aka, F. T., Nagao, K., Kusakabe, M., & Ntepe, N. (2009). Cosmogenic Helium and Neon in Mantle Xenoliths from the Cameroon Volcanic Line (West Africa): Preliminary Observations. *Journal of African Earth Sciences, 55,* 175-184. https://doi.org/10.1016/j.jafrearsci.2009.04.002

Arndt, N. T., Czamanske, G. K., Wooden, J. L., & Fedorenko, V. A. (1993). Mantle and Crustal Contributions to Continental Flood Volcanism. *Tectonophysics, 223,* 39-52. https://doi.org/10.1016/0040-1951(93)90156-E

Ashwal, L. D., & Burke, K. (1989). African Lithospheric Structure, Volcanism, and Topography. *Earth and Planetary Science Letters, 96,* 8-14. https://doi.org/10.1016/0012-821X(89)90119-2

Browne, S. E., & Fairhead, J. D. (1983). Gravity Study of the Central African Rift System: A Model of Continental Disruption 1. The Ngaoundéré and Abu Gabra rifts. *Tectonophysics, 94,* 187-203. https://doi.org/10.1016/0040-1951(83)90016-1

Cai, K., Sun, M., Yuan, C., Zhao, G., Xiao, W., Long, X., & Wu, F. (2010). Geochronological and Geochemical Study of Maic Dykes from the Northwest Chinese Altai: Implications for Petrogenesis and Tectonic Evolution. *Gondwana Research, 18,* 638-652. https://doi.org/10.1016/j.gr.2010.02.010

Cornacchia, M., & Dars, R. (1983). A Major Structural Feature of the African Continent. Central African Lineaments from Cameroon to the Gulf of Aden. *Bulletin de la Société Géologique de France, No. 1,* 101-109. https://doi.org/10.2113/gssgfbull.S7-XXV.1.101

Cox, K. G., & Hawkesworth, C. J. (1985). Geochemical Stratigraphy of the Deccan Traps at Mahabaleshwar, Western Ghats, India, with Implications for Open System Magmatic Processes. *Journal of Petrology, 26,* 355-377. https://doi.org/10.1093/petrology/26.2.355

Déruelle, B., Bardintzeff, J. M., Cheminée, J. L., Ngounouno, I., Lissom, J., Nkoumbou, C., Etamé, J., Hell, J. V., Tanyileke, G., N'ni, J., Ateba, B., Ntepe, N., Nono, A., Wandji, P., Fosso, J., & Nkouathio, D. G. (2000). Simultaneous Eruptions of Alkaline Basalt and

Hawaiite at Mount Cameroon (March 28-April 17, 1999). *Comptes Rendus de l'Académie des Sciences, 331,* 525-531. https://doi.org/10.1016/S1251-8050(00)01454-3

Deruelle, B., Ezangono, J., Lissom, J., Loule, J. P., Ngnotue, N., Ngounouno, I., Nkoumbou, C., Nono, A., & Simo, E. (1987). Mio-Pliocène Basaltic Lava Flows and Phonolitic and Trachytic Plugs North and East of Ngaoundéré (Adamawa, Cameroon). In G. Matheis, & H. Schandelmeier (Eds.), *Current Research in African Earth Sciences* (pp. 261-264). A. A. Balkema.

Déruelle, B., Ngounouno, I., & Demaiffe, D. (2007). The 'Cameroon Hot Line' (CHL): A Unique Example of Active Alkaline Intraplate Structure in Both Oceanic and Continental Lithospheres. *Comptes Rendus Geoscience, 339,* 589-600. https://doi.org/10.1016/j.crte.2007.07.007

Dumont, J. F. (1987). Structural Study of the Northern and Southern Borders of the Adamaoua Plateau: Influence of the Atlantic Context. *Geodynamics, 2,* 55-68.

Ewart, A., Marsh, J. S., Milner, S. C., Duncan, A. R., Kamber, B. S., & Armstrong, R. A. (2004). Petrology and Geochemistry of Early Cretaceous Bimodal Continental Flood Volcanism of the NW Etendeka, Namibia. Part 1: Introduction, Mafic Lavas and Re-Evaluation of Mantle Source Components. *Journal of Petrology, 45,* 59-105. https://doi.org/10.1093/petrology/egg083

Ewart, A., Milner, S. C., Armstrong, R. A., & Duncan, A. R. (1998). Etendeka Volcanism of the Goboboseb Mountains and Messum Igneous Complex, Namibia. Part I: Geochemical Evidence of Early Cretaceous Tristan Plume Melts and the Role of Crustal Contamination in the Paraná-Etendeka CFB. *Journal of Petrology, 39,* 191-225. https://doi.org/10.1093/petroj/39.2.191

Fagny, A. M., Nkouandou, O. F., Déruelle, B., & Ngounouno, I. (2012). Revised Petrology and New Chronological Data on the Peralkaline Felsic Lavas of Ngaoundéré Volcanism (Adamawa Plateau, Cameroon, Central Africa): Evidence of Open-System Magmatic Processes. *Analele Stiintifice ale Universitatii "Al. I. Cuza" din Iasi Seria Geologie, 58,* 5-22.

Fagny, M. A., Nkouandou, O. F., Bardintzeff, J. M., Guillou, H., Iancu, G. O., Njankouo Ndassaa, Z. N., & Temdjim, R. (2020). Petrology and Geochemistry of the Tchabal Mbabo Volcano in Cameroon Volcanic Line (Cameroon, Central Africa): An Intra-Continental Alkaline Volcanism. *Journal of African Earth Sciences, 170,* Article ID: 103832. https://doi.org/10.1016/j.jafrearsci.2020.103832

Fagny, M. A., Nkouandou, O. F., Temdjim, R., Bardintzeff, J. M., Guillou, H., Stumbea, D., & Boutaleb, A. (2016). New K-Ar Ages of Tchabal Mbabo Alcaline Volcano Massif, Cameroun Volcanic Line and Adamawa Plateau (Central Africa). *International Journal of Advanced Geosciences, 4,* 62-71. https://doi.org/10.14419/ijag.v4i2.6516

Fairhead, D., & Okereke, C. S. (1988). Depths to Major Density Contrast beneath the West-African Rift System in Nigeria and Cameroon Based on the Spectral Analysis of Gravity Data. *Journal of African Earth Sciences, 7,* 769-777. https://doi.org/10.1016/0899-5362(88)90018-8

Ferguson, A. K. (1977). The Natural Occurrence of Aegyrine-Neptunite Solid Solution. *Contributions to Mineralogy and Petrology, 60,* 247-253. https://doi.org/10.1007/BF01166799

Fitton, J. G. (1983). Active versus Passive Continental Rifting: Evidence from the West African Rift System. *Tectonophysics, 19,* 473-481. https://doi.org/10.1016/B978-0-444-42198-2.50032-8

Freeth, S. J. (1979). Deformation of the African Plate as a Consequence of Membrane Stress Domains Generated by Post-Jurassic Rift. *Earth and Planetary Science Letters, 45,* 93-104. https://doi.org/10.1016/0012-821X(79)90111-0

Ganwa, A. A., Frisch, W., Siebel, W., Ekodeck, G. E., Cosmas, S. K., & Ngako, V. (2008). Archean Inheritances in the Pyroxene-Amphibole Bearing Gneiss of the Méiganga Area (Central North Cameroon): Geochemical and 207Pb/206Pb Age Imprints. *Comptes Rendus Geoscience, 340,* 211-222. https://doi.org/10.1016/j.crte.2007.12.009

Gèze, B. (1943). Physical Geography and Geology of West Cameroon. *Nouvelles Archives du Muséum d'Histoire Naturelle, 17,* 1-272.

Girod, M. (1968). *The Volcanic Massif of Atakor (Hoggar, Algerian Sahara). Petrological, Structural and Volcanological Study.* Ph.D. Thesis, University of Paris-Sud, 401 p.

Gouhier, J., Nougier, J., & Nougier, D. (1974). Contribution to the Volcanology Study of Cameroon (Cameroon Line-Adamawa). *Annales de la Faculté des Sciences du Cameroun, 17,* 3-49.

Green, D. H. (1973). Experimental Melting Studies on a Model Upper Mantle Composition at High Pressure under Water-Saturated and Water-Undersaturated Conditions. *Earth and Planetary Science Letters, 19,* 37-53. https://doi.org/10.1016/0012-821X(73)90176-3

Guiraud, R., Binks, R. M., Fairhead, J. D., & Wilson, M. (1992). Chronology and Geodynamic Setting of Cretaceous-Cenozoic Rifting in West and Central Africa. *Tectonophysics, 213,* 227-234. https://doi.org/10.1016/B978-0-444-89912-5.50039-9

Guiraudie, C. (1955). *Geological Reconnaissance Map at the Scale of 1/50000; Territory of Cameroon Ngaoundéré West.* Sers. Mine Cam, Paris, 1 Map and Leaflet 23 p.

Kamgang, P., Chazot, G., Njonfang, E., & Tchoua, F. (2008). Geochemistry and Geochronology of Mafic Rocks from Bamenda Mountains (Cameroon): Source Composition and Crustal Contamination along the Cameroon Volcanic Line. *Comptes Rendus Geoscience, 340,* 850-857. https://doi.org/10.1016/j.crte.2008.08.008

Kamgang, P., Njonfang, E., Nono, A., Gountie, D. M., & Tchoua, F. (2010). Petrogenesis of a Silicic Magma System: Geochemical Evidence from Bamenda Mountains, NW Cameroon, Cameroon Volcanic Line. *Journal of African Earth Sciences, 58,* 285-304. https://doi.org/10.1016/j.jafrearsci.2010.03.008

Kampunzu, A. B., & Popoff, M. (1991). Distribution of the Main Phanerozoic African Rifts and Associated Magmatism: Introductory Notes. In A. B. Kampunzu, & R. T. Lubala (Eds.), *Magmatism in Extensional Structural Settings, the Phanerozoic African Plate* (pp. 2-10). Springer-Verlag. https://doi.org/10.1007/978-3-642-73966-8_1

Lasserre, M. (1961). Etude geologique de la partie orientale de l'Adamaoua (Cameroun Central) et les principales sources mineralisées de l'Adamaoua. *Bulletin de la Direction des Mines et Geologie du Cameroun, 4,* 1-131.

Le Bas, M. J., Le Maitre, R. W., Streickeisen, A., & Zanettin, B. (1986). A Chemical Classification of Volcanic Rocks Based on the Total Alkali-Silica Diagram. *Journal of Petrology, 27,* 745-750. https://doi.org/10.1093/petrology/27.3.745

Le Maréchal, A., & Vincent, P. M. (1971). Le Fossé Crétacé du Sud Adamaoua (Cameroun). *Cahier d'ORSTOM Série Géologique, 3,* 67-83.

Marzoli, A., Renne, P. R., Piccirillo, E. M., Francesca, C., Bellieni, G., Melfi, A. J., Nyobe, J. B., & N'ni, J. (1999). Silicic Magmas from the Continental Cameroon Volcanic Line (Oku, Bambouto and Ngaoundere): ^{40}Ar-^{39}Ar Dates, Petrology, Sr-Nd-O Isotopes and Their Petrogenetic Significance. *Contributions to Mineralogy and Petrology, 135,* 133-150. https://doi.org/10.1007/s004100050502

Mbowou, G. I. B., Ngounouno, I., & Déruelle, B. (2010). Petrology of the Bimodal Volcanism of Djinga Tadorgal (Adamaoua, Cameroon). *Revue CAMES-Series A, 11,* 36-42.

McDonough, W. F., & Sun, S. S. (1995). The Composition of the Earth. *Chemical Geology, 120,* 223-253. https://doi.org/10.1016/0009-2541(94)00140-4

Ménard, J. J., Wandji, P., Déruelle, B., & Ezangono Tolo, J. M. (1998). The Djinga Volcano (Adamaoua-Cameroon): Geology and Petrography. In *Geosciences in Cameroon, Collect. GEOCAM, 1/1998* (pp. 185-190).

Moreau, C., Regnoult, J. M., Déruelle, B., & Robineau, B. (1987). A New Tectonic Model for the Cameroon Line, Central Africa. *Tectonophysics, 139,* 317-334. https://doi.org/10.1016/0040-1951(87)90206-X

Morimoto, N., Fabriès, J., Ferguson, A. K., Ginzburg, I. V., Ross, M., Seifert, F. A., Zussman, J., Aoki, K., & Gottardi, G. (1988). Nomenclature of Pyroxenes. *Mineralogical Magazine, 52,* 535-550. https://doi.org/10.1180/minmag.1988.052.367.15

Ngako, V., Njonfang, E., Aka, F. T., Affaton, T., & Nnange, J. M. (2006). The North-South Paleozoic to Quaternary Trend of Alkaline Magmatism from Niger-Nigeria to Cameroon: Complex Interaction between Hotspot and Precambrian Faults. *Journal or African Earth Sciences, 45,* 241-256. https://doi.org/10.1016/j.jafrearsci.2006.03.003

Ngangom, E. (1983). Etude tectonique du fossée de la Mbéré et du Djerem, Sud Adamaoua. *Bulletin des Centres de Recherches Exploration-Production Elf-Aquitaine, 7,* 339-347.

Ngounouno, I., Déruelle, B., & Demaiffe, D. (2000). Petrology of the Bimodal Cenozoic Volcanism of the Kapsiki Plateau (Northern Most Cameroon, Central Africa). *Journal of Volcanology and Geothermal Research, 102,* 21-44. https://doi.org/10.1016/S0377-0273(00)00180-3

Ngounouno, I., Déruelle, B., Montigny, R., & Demaiffe, D. (2006). Camptonites of Mount Cameroon, Africa. *Comptes Rendus Geoscience, 338,* 537-544. https://doi.org/10.1016/j.crte.2006.03.015

Ngwa, C. N., Shu, B. N., Mbassa, B. J., Aka, F. T., & Wokwenmendam, P. N. (2019). Olivine Chemistry from Cameroon Evidence of Carbonate Metasomatism along the Ocean-Continental of the Cameroon Volcanic Line. *Mineralogy and Petrology, 114,* 57-70. https://doi.org/10.1007/s00710-019-00689-5

Nielsen, L. E. (1979). Dynamic Mechanical Properties of Polymers Filled with Agglomerated Particles. *Journal of Polymer Science, 17,* 1897-1901. https://doi.org/10.1002/pol.1979.180171106

Nkouandou, O. F., & Temdjim, R. (2011). Petrology of Spinel Lherzolite Xenoliths and Host Basaltic Lava from Nga Voglar Volcano, Adamawa Massif (Cameroon Volcanic Line, West Africa): Equilibrium Conditions and Mantle Characteristics. *Journal of Geosciences, 56,* 375-387. http://doi.org/10.3190/jgeosci.108

Nkouandou, O. F., Fagny, A. M., Iancu, G. O., & Bardintzeff, J. M. (2015). Petrology and Geochemistry of Doleritic Dyke of Likok (Cameroon, Central Africa). *Carpathian Journal of Earth and Environmental Sciences, 10,* 121-132.

Nkouandou, O. F., Ngounouno I., & Déruelle, B. (2010). Geochemistry of Recent Basaltic Lavas from the North and East of Ngaoundéré Zones (Cameroon, Adamawa Plateau, Central Africa): Petrogenesis and the Nature of the Source. *International Journal of Biological and Chemical Sciences, 10,* 1903-1917. https://doi.org/10.4314/ijbcs.v10i4.38

Nkouandou, O. F., Ngounouno, I., Déruelle, B., Onhenstetter, D., Montigny, R., & Demaiffe, D. (2008). Petrology of the Mio-Pliocene Volcanism to the North and East of Ngaoundéré (Adamawa-Cameroon). *Comptes Rendus Geoscience, 340,* 28-37. https://doi.org/10.1016/j.crte.2007.10.012

Nono, A., Déruelle, B., Demaiffe, D., & Kambou, R. (1994). Tchabal Nganha Volcano in

Adamawa (Cameroon): Petrology of a Continental Alkaline Lava Series. *Journal of Volcanology and Geothermal Research, 60,* 147-178. https://doi.org/10.1016/0377-0273(94)90066-3

Okereke, C. S. (1988). Contrasting Modes of Rifting: The Benue Trough and Cameroon Volcanic Line, West Africa. *Tectonophysics, 7,* 775-784. https://doi.org/10.1029/TC007i004p00775

Oustriere, P. (1984). *Geological and Geochemical Study of the Lake Basin of Anloua (Cameroon). Application to Understanding the Genesis of Vivianite.* Ph.D. Thesis, University of Orleans, 344 p.

Poudjom Djomani, Y. H., Diament, M., & Wilson, M. (1997). Lithospheric Structures across the Adamawa Plateau (Cameroon) from Gravity Studies. *Tectonophysics, 273,* 317-327. https://doi.org/10.1016/S0040-1951(96)00280-6

Roeder, P. L., & Emslie, R. F. (1970). Olivine-Liquid Equilibrium. *Contributions to Mineralogy and Petrology, 29,* 275-289. https://doi.org/10.1007/BF00371276

Tchop, L. J., Wokwenmendam, P. N., Ntieche, B., Metang, V., Dili Rake, J., Teitchou, M. I., Auwera, J. V., Ekodeck, G., & Nkoumbou, C. (2020). New Data on the Genesis and Evolution of the Primitive Magmas of Mount Cameroon: Contribution of Melt Inclusions. *Journal of Geological Research, 2*, Article ID: 2308. https://doi.org/10.30564/jgr.v2i4.2308

Temdjim, R. (2012). Ultramafic Xenoliths from Lake Nyos Area, Cameroon Volcanic Line, West-Central Africa: Petrography, Mineral Chemistry, Equilibration Conditions and Metasomatic Features. *Chemie der Erde—Geochemistry, 72,* 39-60. https://doi.org/10.1016/j.chemer.2011.07.00

Temdjim, R., Njilah, I. K., Kamgang, P., & Nkoumbou, C. (2004). New Data on the Felsic Lavas of Ngaoundéré (Adamaoua, Cameroon Line): K-Ar Chronology and Petrology. *African Journal of Science and Technology, 5,* 113-123.

Toteu, S. F., Penaye, J., & Djomani, Y. P. (2004). Geodynamic Evolution of the Pan-African Belt in Central Africa with Special Reference to Cameroon. *Canadian Journal of Earth Sciences, 41,* 73-85. https://doi.org/10.1139/e03-079

Wandji, P., Tsafack, J. P. F., Bardintzeff, J. M., Nkouathio, D. G., Kagoudongmo, A., Bellon, H., & Guillou, H. (2009). Xenoliths of Dunites, Wehrlites and Clinopyroxenite in the Basanites from Batoke Volcanic Cone (Mount Cameroon, Central Africa): Petrogenetic Implications. *Mineralogy and Petrology, 96,* 81-98. https://doi.org/10.1007/s00710-008-0040-3

Wass, S. Y. (1979). Multiple Origins of Clinopyroxenes in Alkali Basaltic Rocks. *Lithos, 12,* 115-132. https://doi.org/10.1016/0024-4937(79)90043-4

Weaver, B. L., & Tarney, J. (1984). Empirical Approach to Estimating the Composition of the Continental Crust. *Nature, 310,* 575-577.

Zhao, J. X., McCulloch, M. T., & Korsch, R. J. (1994). Characterisation of a Plume-Related~800 Ma Magmatic Event and Its Implications for Basin Formation in Central-Southern Australia. *Earth and Planetary Science Letters, 121,* 349-367. https://doi.org/10.1016/0012-821X(94)90077-9